iScience

CellPress
OPEN ACCESS

Article

ORF8 contributes to cytokine storm during SARS-CoV-2 infection by activating IL-17 pathway

Xiaoyuan Lin,[1,11] Beibei Fu,[1,11] Songna Yin,[2,11] Zhifeng Li,[3] Huawen Liu,[4] Haiwei Zhang,[5] Na Xing,[6] Yu Wang,[7] Weiwei Xue,[8] Yan Xiong,[1] Shanfu Zhang,[1] Qingting Zhao,[1] Shiyao Xu,[1] Jing Zhang,[9] Peihui Wang,[9] Weiqi Nian,[5,*] Xingsheng Wang,[10,*] and Haibo Wu[1,12,*]

SUMMARY

Recently, COVID-19 caused by the novel coronavirus SARS-CoV-2 has brought great challenges to the world. More and more studies have shown that patients with severe COVID-19 may suffer from cytokine storm syndrome; however, there are few studies on its pathogenesis. Here we demonstrated that SARS-CoV-2 coding protein open reading frame 8 (ORF8) acted as a contributing factor to cytokine storm during COVID-19 infection. ORF8 could activate IL-17 signaling pathway and promote the expression of pro-inflammatory factors. Moreover, we demonstrated that treatment of IL17RA antibody protected mice from ORF8-induced inflammation. Our findings are helpful to understand the pathogenesis of cytokine storm caused by SARS-CoV-2 and provide a potential target for the development of COVID-19 therapeutic drugs.

INTRODUCTION

Coronavirus disease 2019 (COVID-19) is a respiratory infectious disease caused by severe acute respiratory syndrome coronavirus 2 (SARS-CoV-2). At present, it is still a worldwide epidemic with nearly 24 million people infected, which has brought severe challenges to global public health. The clinical course of patients remains to be fully characterized, and no pharmacological therapies of proven efficacy yet exist (Russell et al., 2020). To open up a new breakthrough for clinical therapy, it is necessary to uncover the pathogenesis from a perspective of host-microbe interaction. However, except for a certain understanding of Spike protein (Walls et al., 2020), other proteins' functions have not been extensively studied. In this study, we demonstrated that open reading frame 8 (ORF8) could activate IL-17 signaling pathway and promote the expression of pro-inflammatory factors by interacting with host IL17RA. We also found that inhibition of this interaction by IL17RA antibody was helpful to control the cytokine storm in SARS-CoV-2 infection. Our findings not only made an important contribution to the understanding of how various effectors of the immune system initiate the cytokine storm but also provided a potential target for the development of COVID-19 therapeutic drugs.

RESULTS

ORF8 promotes the secretion of inflammatory factors by activating IL-17 signaling pathway

According to clinical data analysis, patients with severe COVID-19 showed cytokine storm, resulting in acute respiratory distress syndrome (ARDS) and multiple organ failure (Mangalmurti and Hunter, 2020; Vaninov, 2020). Cytokine storm refers to the rapid production of many cytokines, such as TNF-α, IL-1, IL-6, IL-12, and IFN-α. ARDS caused by cytokine storm in the late stage of infection is an important node in the transition from mild to severe illness, and it is also an important cause of death (Wu et al., 2020). In the current treatment of COVID-19, antibodies targeting IL-6 are commonly used to inhibit cytokine storm. However, suppression of IL-6 has not achieved a desired effect in clinical treatment (Hermine et al., 2021; Salama et al., 2021; Stone et al., 2020). As a proinflammatory cytokine, IL-17 has been reported to be related to cytokine storm (Crowe et al., 2009; Kolls and Lindén, 2004). Targeting IL-17 is immunologically plausible as a strategy to prevent ARDS in COVID-19 (Orlov et al., 2020; Pacha et al., 2020). In this study, yeast two-hybrid system was used to screen the SARS-CoV-2 proteins that interacted with IL-17 receptors. Three candidates (NSP2, ORF7a, and ORF8) were obtained through yeast two-hybrid experiment (Figure S1), and

[1]School of Life Sciences, Chongqing University, Chongqing 401331, China

[2]Medical school, Yan'an University, Yan'an, 716000 Shaanxi, China

[3]Chongqing Center for Disease Control and Prevention, Chongqing 400042, China

[4]Affiliated Three Gorges Hospital of Chongqing University, Chongqing Three Gorges Central Hospital, Chongqing 404100, China

[5]Chongqing Key Laboratory of Translational Research for Cancer Metastasis and Individualized Treatment, Chongqing University Cancer Hospital, Chongqing 400030, China

[6]Institut für Virologie, Freie Universität Berlin, Robert-von-Ostertag-Str. 7-13, 14163 Berlin, Germany

[7]Technical Center of Chongqing Customs, Chongqing 401147, China

[8]School of Pharmaceutical Sciences, Chongqing University, Chongqing 401331, China

[9]Advanced Medical Research Institute, Cheeloo College of Medicine, Shandong University, Jinan, Shandong 250012, China

[10]Department of Respiratory Medicine, Affiliated Central Hospital of Chongqing University, Chongqing Emergency Medical Center, Chongqing 400014, China

[11]These authors contributed equally

[12]Lead contact

*Correspondence: nwqone@126.com (W.N.), shengxw73@163.com (X.W.), hbwu023@cqu.edu.cn (H.W.)

https://doi.org/10.1016/j.isci.2021.102293

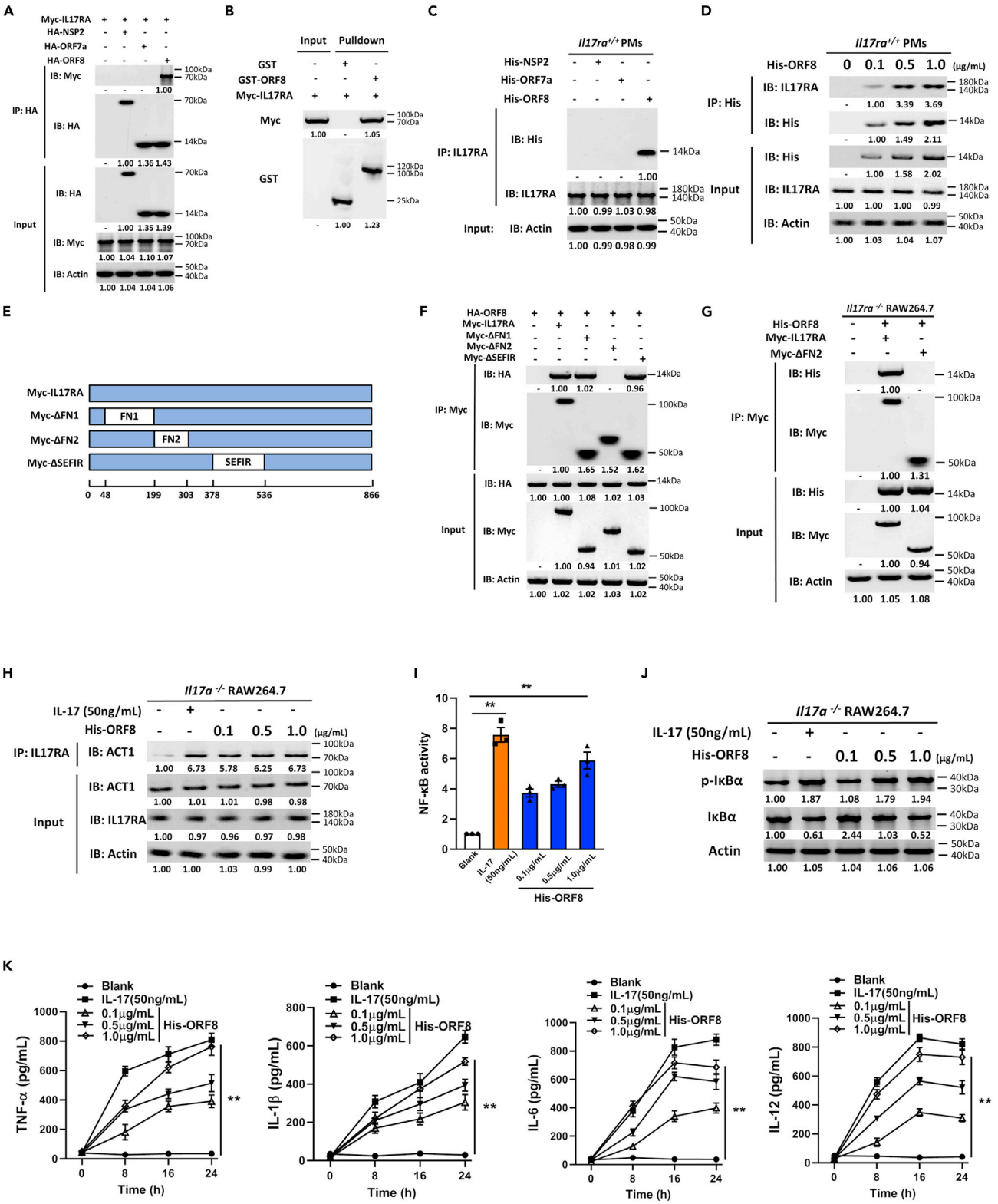

Figure 1. ORF8 promotes the secretion of inflammatory factors by activating IL-17 pathway

(A) HEK293T cells were co-transfected with Myc-IL17RA and HA-NSP2/HA-ORF7a/HA-ORF8 for 24 h, and the interaction of IL17RA with NSP2/ORF7a/ORF8 was detected by immunoprecipitation.

Figure 1. *Continued*

(B) GST pulldown analysis of the interaction between GST-ORF8 and Myc-IL17RA.

(C) *Il17ra*$^{+/+}$ PMs were treated with 1 μg/mL His-tagged NSP2/ORF7a/ORF8 for 24 h, and immunoprecipitation was performed to detect the interaction of IL17RA with NSP2/ORF7a/ORF8.

(D) *Il17ra*$^{+/+}$ PMs were treated with different concentrations of purified His-ORF8 protein for 24 h, and immunoprecipitation was performed to detect the interaction of IL17RA with ORF8.

(E) Schematic diagram of IL17RA truncations.

(F and G) Co-immunoprecipitation analysis of the interaction between ORF8 and IL17RA truncations in HEK293T cells co-transfected with HA-ORF8 and truncation plasmids for 24 h (F), or in *Il17ra*$^{-/-}$ RAW264.7 transfected with IL17RA truncation plasmids for 24 h, and treated with 1 μg/mL His-ORF8 protein for 24 h (G).

(H–K) *Il17a*$^{-/-}$ RAW264.7 were treated with 50 ng/mL IL-17 or 0.1–1 μg/mL His-ORF8 protein as indicated for 24 h. The interaction between IL17RA and ACT1 was detected by co-immunoprecipitation (H); NF-κB activity was detected by dual luciferase reporter analysis (I); phosphorylation level of IκBα was detected by western blotting (J); and secretion of TNF-α, IL-1β, IL-6, and IL-12 was detected by ELISA analysis (K).

Data are representative of three independent experiments (A–D, F–H, and J) or three independent experiments with n = 3 technical replicates (I and K) (shown as mean ± SEM in I and K). Individual data points represent individual technical replicates (I). Data are analyzed by two-tailed Student's t test (I and K). **$p < 0.01$.

the interaction was further examined by immunoprecipitation experiments. As a result, only the interaction between ORF8 and IL17RA was successfully verified (Figure 1A), which is consistent with the predicted SARS-CoV-2 protein interaction map (Gordon et al., 2020). It has been reported that ORF8 is associated with COVID-19 severity (Young et al., 2020). Patients infected with the ORF8 mutant (Δ382-variant) of SARS-CoV-2 had lower concentrations of pro-inflammatory cytokines and chemokines (Young et al., 2020), indicating an important role of ORF8 in the study of cytokine storm caused by COVID-19. We further validated the interaction between ORF8 and IL17RA using GST pulldown assay and proved an *in vitro* interaction of ORF8 and IL17RA (Figure 1B). As IL17RA is an important receptor mainly expressed in immune cells (Lore et al., 2016), *in vitro* purified His-ORF8 protein was supplemented into wild-type mouse peritoneal macrophages (*Il17ra*$^{+/+}$ PMs) to further validate its interaction with IL17RA. The results showed that ORF8 interacted with endogenous IL17RA, and this interaction was in a dose-dependent manner (Figures 1C and 1D). These evidences indicated that SARS-CoV-2 ORF8 protein interacted with host receptor IL17RA.

We then constructed domain truncations of IL17RA to investigate the IL17RA-ORF8 interaction (Figure 1E). IL17RA is composed of three main functional domains: fnIII_D1, fnIII_D2, and SEFIR. In HEK293T cells, co-immunoprecipitation showed that deletion of fnIII-D2 domain in IL17RA impaired IL17RA-ORF8 interaction (Figure 1F). Furthermore, we transfected IL17RA or fnIII_D2 domain truncation into *Il17ra*-deficient RAW264.7 cells (*Il17ra*$^{-/-}$ RAW264.7) (Figure S2) and treated cells with ORF8 protein. The results showed that ORF8 could interact with the complete IL17RA, instead of the truncation lacking fnIII_D2 domain (Figure 1G). Taken together, these results indicated that the binding of ORF8 to host IL17RA is fnIII_D2 domain dependent.

IL-17 pathway is an important pro-inflammatory signaling in mammals (McGeachy et al., 2019). IL-17 ligand binds to and activates the corresponding receptor, and then the complex recruits ACT1 from the cytoplasm through the SEFIR domain. ACT1 initiates TNF receptor-associated factor 6 (TRAF6) to activate NF-κB signaling pathway, thus improving the expression levels of pro-inflammatory factors (Schwandner et al., 2000). Given the fact that ORF8 interacts with IL17RA, we investigated the effect of ORF8 on IL-17 pathway. To eliminate the possibility that ORF8 directly influences the expression of IL-17, we generated *Il17a*-deficient RAW264.7 cells (*Il17a*$^{-/-}$ RAW264.7) (Figure S3) and *Il17a*-deficient mouse models (Figure S4). After ORF8 treatment, it was found that ACT1 was recruited by IL17RA, and the recruitment effect was not significantly affected by ORF8 concentrations (Figure 1H). However, a dose-dependent activation in NF-κB signaling pathway was observed in *Il17a*$^{-/-}$ RAW264.7 (Figures 1I and 1J). In addition, a dose-dependent manner in cytokine TNF-α, IL-1β, IL-6, and IL-12 release was identified (Figure 1K). Taken together, these results implied that ORF8 could bind to IL17RA receptor, leading to IL-17 pathway activation and an increased secretion of pro-inflammatory factors.

Inhibition of IL-17 pathway protects mice from ORF8-induced inflammation

We further explored methods for blocking the ORF8-induced IL-17 pathway activation using IL17RA antibody. Compared with the isotype control, the activity of NF-κB signaling pathway was significantly inhibited after IL17RA antibody treatment (Figure 2A). Similarly, the secretion of cytokines, such as TNF-α,

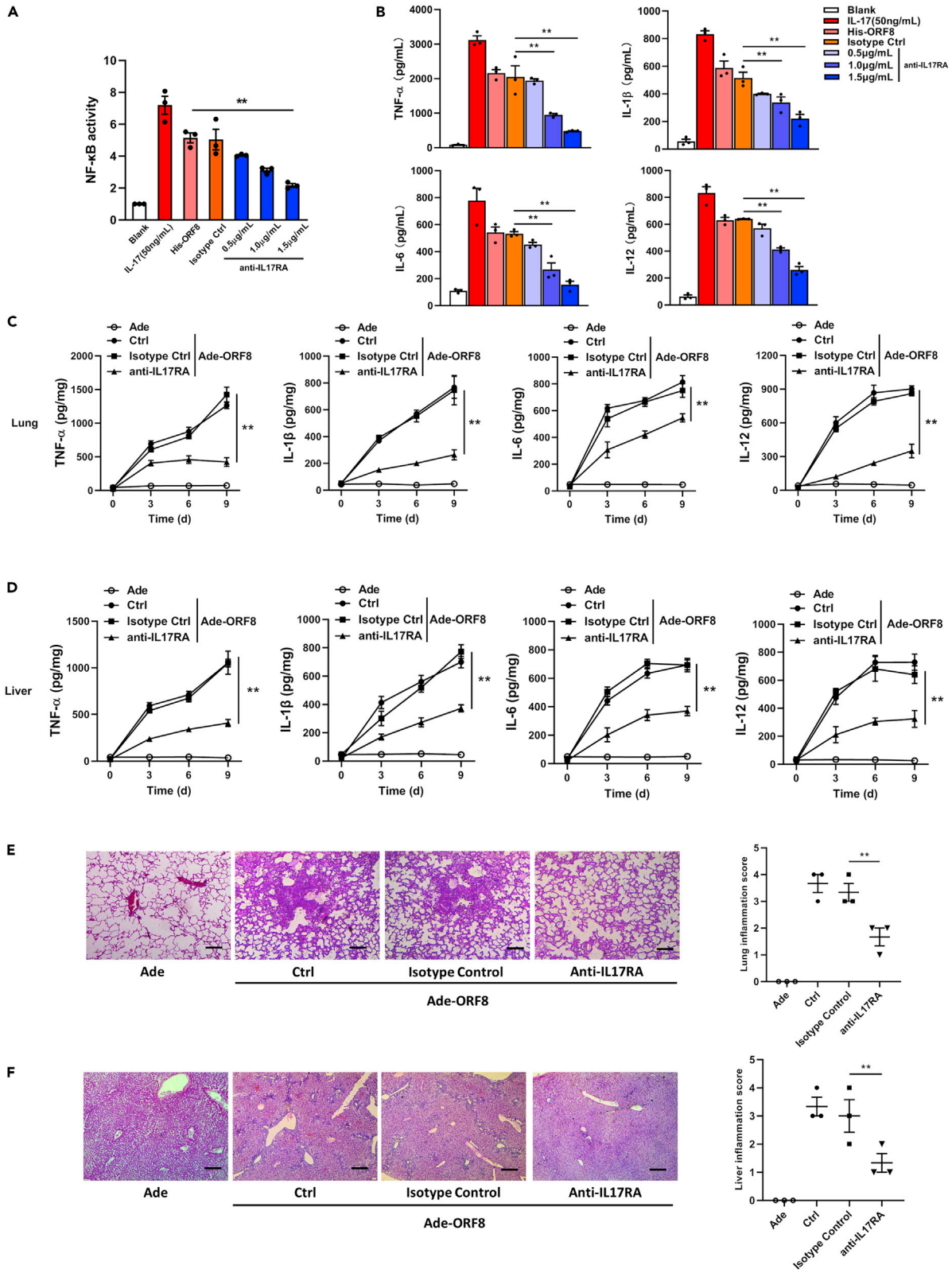

Figure 2. IL17RA antibody protects mice from ORF8-induced inflammation

(A and B) *Il17a*$^{-/-}$ RAW264.7 were treated with IL17RA antibody as indicated for 8 h and treated by 1 μg/mL His-ORF8 protein for 24 h. NF-κB activity was detected by dual luciferase reporter analysis (A), and the secretion of TNF-α, IL-1β, IL-6, and IL-12 was detected by ELISA (B). Blank: negative control; IL-17:

Figure 2. *Continued*

cells were treated with 50 ng/mL IL-17 for 24 h; His-ORF8: cells were treated with 1 μg/mL His-ORF8 for 24 h; Isotype Ctrl: cells were treated with Isotype antibody of IL17RA for 8 h and further treated by 1 μg/mL His-ORF8 protein for 24 h.

(C and D) *Il17a*-deficient C57BL/6 mice were intraperitoneally injected with 200 μg IL17RA antibody, and the injection was repeated every 3 days. After the second injection, mice were intratracheally infected with the adenovirus expressing ORF8 (10^8 PFU/mouse). The time was recorded as day 0. Afterward, lung (C) and liver (D) sections were taken every 3 days. The secretion of TNF-α, IL-1, IL-6, and IL-12 was detected by ELISA.

(E and F) H&E staining in lung (E) and liver (F) sections on day 9 post-infection. The degree of organ damage was assessed by a scoring system. Scale bar, 400 μm.

Data are representative of three independent experiments (E and F) or three independent experiments with n = 3 technical replicates (A–F) (shown as mean ± SEM in A–F). Individual data points represent individual technical replicates (A, B, E, and F). Data are analyzed by two-tailed Student's t test (A–F). $^{**}p < 0.01$.

IL-1β, IL-6, and IL-12, was also reduced to varying degrees according to concentration gradient of IL17RA antibody (Figure 2B). To study the effect of ORF8 on inflammation, we packaged a pseudovirus expressing ORF8 by using adenovirus. *Il17a*-deficient mice were infected with 10^8 plaque-forming unit (PFU) pseudoviruses through intratracheal infection. qRT-PCR results of lung and liver showed that ORF8 was stably expressed in mice within 9 days after injection (Figure S5). Meanwhile, IL-17 receptors were blocked by intraperitoneal injection with IL17RA antibody. As a result, the secretion of pro-inflammatory factors in lung continued to increase after ORF8 pseudovirus infection in the isotype control groups (Figure 2C). However, for the mice injected with IL17RA antibody, although the secretion of pro-inflammatory factors increased, the total amount was much lower compared with that of the isotype control (Figure 2C). Liver, another organ with a high rate of impairment in patients with severe COVID-19 (Zhang et al., 2020a), showed a similar trend as lung during ORF8 pseudovirus infection (Figure 2D). In addition, by using H&E staining and a scoring system, we observed a histological damage on day 9 post-infection. Lungs and livers of the mice injected with IL17RA antibody underwent a slight inflammation compared with those of the untreated mice (Figures 2E and 2F). Collectively, our study indicated that SARS-CoV-2 coding protein ORF8 might be a contributing factor to the cytokine storm during COVID-19 and treatment with IL17RA antibody could protect organs from inflammation and damage.

DISCUSSION

The control of cytokine storm has always been a difficulty in clinical therapy. At present, studies on SARS-CoV-2 have basically clarified the mechanisms of viral invasion (Hoffmann et al., 2020; Shang et al., 2020), whereas the process of viral replication, viral release, and host immune regulation still needs in-depth exploration. Here, we identified that SARS-CoV-2 ORF8 emulated the function of IL-17 by interacting with host IL17RA, and then promoted the secretion of pro-inflammatory factors by activating NF-κB signaling pathway. To eliminate the possibility that ORF8 stimulates the expression of endogenous IL-17, we generated *Il17a*$^{-/-}$ cells and mouse models. Supplementation of either IL-17 or ORF8 to *Il17a*$^{-/-}$ RAW264.7 activated NF-κB pathway, indicating an independent role of ORF8 in promoting inflammation.

In this study, we found that ORF8 protein acted as a contributing factor to the cytokine storm by inducing IL-17 signaling pathway, and the interaction between ORF8 and IL17RA was pivotal in the progress of inflammation. However, two questions remain unanswered. First, IL17RA is a transmembrane protein (Lore et al., 2016), and we found that ORF8 bound to the extracellular domain of IL17RA. It is unclear how the virus exposes ORF8 and interacts with IL17RA. Second, SARS-CoV-2 invades alveolar epithelial cells mainly through ACE2 receptors on the cell surface (Hoffmann et al., 2020). However, monocytes/macrophages play a more critical role in the secretion and regulation of cytokines. Interestingly, due to the low abundance of ACE2 receptors on the surface, monocytes/macrophages are not the main targets of the virus (Kuba et al., 2010). Therefore, the question is how the virus achieves communication from the alveolar epithelial cells to the monocytes/macrophages. A fact that has caught our attention is that clinical cases have shown that the viral loads in patients are not directly proportional to the severity of disease symptoms (Lescure et al., 2020; To et al., 2020). This indicates the possible existence of a unique indirect cellular communication mechanism (not by virion release) in the occurrence and development of cytokine storm. Chan et al. suggested that ORF8 might be a secretory protein of SARS-CoV-2 that can be released outside the cell (Chan et al., 2020). Previous studies have demonstrated that certain viruses can secrete virulence factors to manipulate host cell machinery, thus allowing infection, survival, or replication of pathogens (McNamara et al., 2018; Mukhamedova et al., 2019; Nordholm et al., 2017). For example, HIV only infects a limited repertoire of cells expressing HIV receptors. However, the HIV protein NEF released from infected cells in extracellular vesicles can be taken up by uninfected cells, thereby impairing cholesterol metabolism in these cells. This impairment causes the formation of excessive lipid rafts and re-localization of the inflammatory

receptors into rafts and triggers inflammation (Mukhamedova et al., 2019). In a recent study, ORF8 has been shown to interact with MHC-I (Zhang et al., 2020b), which is one of the marker proteins located on the surface of exosomal membranes (Becker et al., 2016). If ORF8 interacts with MHC-I and appears on the surface of exosomal membranes, it will increase the possibility that ORF8 protein interacts with the extracellular domain of IL-17 receptor and subsequently activates the NF-κB signaling pathway and increases the transcription of cytokines. In this way, ORF8 protein achieves being transmitted from alveolar epithelial cells to monocytes/macrophages, thereby leading to the outbreak of cytokine storm. Transwell system has been reported to study cellular communications in different studies, such as the communication between dendritic cells and endothelial cells (Gao et al., 2016), nerve cells and microglial cells (Yin et al., 2020), and even the triple interaction of epithelial cells, endothelial cells, and THP-1 cells (Costa et al., 2019). It would be interesting to construct an epithelial cell-macrophage co-culture system using a Transwell model, so as to study the transmission process of ORF8 from epithelial cells to macrophages.

ORF8 also has an inhibitory effect on the interferon pathway (Li et al., 2020; Rao et al., 2021), and Blanco-Melo et al. have reported that reduced interferon pathway coupled with exuberant inflammatory cytokine production are the defining and driving features of COVID-19 (Blanco-Melo et al., 2020). In a recent study, Miorin et al. have showed that ORF6 has the effect of antagonizing interferon signaling (Miorin et al., 2020), whereas we have found that ORF8 has the effect of promoting inflammatory cytokine production. This is consistent with the study of Blanco-Melo et al. Therefore, we speculate that the roles of these ORFs may be opposing, which also makes the pathogenesis of SARS-CoV-2 more complicated than that of common respiratory viruses. In our current work, we have proved that the binding of IL17RA with ORF8 depends on the fnIII_D2 domain of IL17RA and the binding site in ORF8 has not been determined. Young et al. found that Δ382-variant infection tended to be milder compared with those caused by the wild-type virus, with less pronounced cytokine release during the acute phase of infection (Young et al., 2020). Considering that the interaction between ORF8 and IL17RA has an important contribution in improving the expression of pro-inflammatory factors, we speculate that Δ382 variant might show a reduced ability to interact with IL17RA, which, however, needs to be verified with further experiments.

As a universal subunit of the IL-17 receptor family, IL17RA participates in the assembly of almost all the receptor complexes (Li et al., 2019), providing a broader site for ORF8 binding. However, it is worth considering that the other members of IL-17 receptor family have a similar structure to IL17RA, which may also be potential binding targets of ORF8. It has been reported that orphan receptor IL17RD can regulate various pathways employed by IL-17A in different ways (Mellett et al., 2012). The lack of IL17RD in cells leads to an enhancement in pre-inflammatory signals (Mellett et al., 2015). If ORF8 interacts with orphan IL17RD, the ORF8-IL17RD complex could disrupt the interaction between ACT1 and TRAF6. In this way, there will be a different regulatory mechanism existed, and further studies on this could be interesting.

Limitations of study

In this study, we found that ORF8 protein of SAR-CoV-2 can activate IL-17 signaling pathway by interacting with IL17RA, thereby up-regulating the secretion of inflammatory factors. Treatment with IL17RA antibody can protect mice from inflammatory damages caused by ORF8. However, as we have discussed in the article, IL17RA is a transmembrane protein, and the way in which ORF8 interacts with its extracellular domain is unclear. In addition, the main findings of this article should be further clarified using SARS-CoV-2 live virus instead of pseudovirus.

Resource availability

Lead contact

Further information and requests for resources should be directed to and will be fulfilled by the lead contact, Haibo Wu (hbwu023@cqu.edu.cn).

Materials availability

This study did not generate new unique reagents.

Data and code availability

Yeast two-hybrid screening data associated with this study are available from "Mendeley Data: https://doi.org/10.17632/ty66rbxkk8.1."

METHODS

All methods can be found in the accompanying transparent methods supplemental file.

SUPPLEMENTAL INFORMATION

Supplemental Information can be found online at https://doi.org/10.1016/j.isci.2021.102293.

ACKNOWLEDGMENTS

This work was supported by the National Natural Science Foundation of China, SGC's Rapid Response Funding for COVID-19 (No.C-0002), the National Natural Science Foundation of China (No. 81970008, 31702205), the Fundamental Research Funds for the Central Universities (No. 2019CDYGZD009, 2020CDJYGRH-1005, and 2019CDYGYB005), and the Natural Science Foundation of Chongqing, China (No. cstc2020jcyj-msxmX0460 and cstc2020jcyj-bsh0055). The funders had no role in study design, data collection, and analysis, decision to publish, or preparation of the manuscript.

AUTHOR CONTRIBUTIONS

H.W., W.N., X.W., and X.L. conceived and designed the study. H.W., X.L., B.F., S.Y., Z.L., H.L., H.Z., N.X., Y.W., W.X., Y.X., S.Z., Q.Z., S.X., X.W. performed the experiments. P.W. and J.Z. helped with plasmids construction. H.W., S.Y., B.F., and X.L. analyzed the data. H.W., X.L., and B.F. wrote the manuscript. All authors read and approved the final manuscript.

DECLARATION OF INTERESTS

The authors declare no competing interests.

Received: October 1, 2020
Revised: January 29, 2021
Accepted: March 5, 2021
Published: April 23, 2021

REFERENCES

Becker, A., Thakur, B.K., Weiss, J.M., Kim, H.S., Peinado, H., and Lyden, D. (2016). Extracellular vesicles in cancer: cell-to-cell mediators of metastasis. Cancer Cell *30*, 836–848.

Blanco-Melo, D., Nilsson-Payant, B.E., Liu, W.C., Uhl, S., Hoagland, D., Moller, R., Jordan, T.X., Oishi, K., Panis, M., Sachs, D., et al. (2020). Imbalanced host response to SARS-CoV-2 drives development of COVID-19. Cell *181*, 1036–1045 e1039.

Chan, J.F., Kok, K.H., Zhu, Z., Chu, H., To, K.K., Yuan, S., and Yuen, K.Y. (2020). Genomic characterization of the 2019 novel human-pathogenic coronavirus isolated from a patient with atypical pneumonia after visiting Wuhan. Emerg. Microb. Infect. *9*, 221–236.

Costa, A., de Souza Carvalho-Wodarz, C., Seabra, V., Sarmento, B., and Lehr, C.M. (2019). Triple co-culture of human alveolar epithelium, endothelium and macrophages for studying the interaction of nanocarriers with the air-blood barrier. Acta Biomater. *91*, 235–247.

Crowe, C.R., Chen, K., Pociask, D.A., Alcorn, J.F., Krivich, C., Enelow, R.I., Ross, T.M., Witztum, J.L., and Kolls, J.K. (2009). Critical role of IL-17RA in immunopathology of influenza infection. J. Immunol. *183*, 5301–5310.

Gao, W., Liu, H., Yuan, J., Wu, C., Huang, D., Ma, Y., Zhu, J., Ma, L., Guo, J., Shi, H., et al. (2016). Exosomes derived from mature dendritic cells increase endothelial inflammation and atherosclerosis via membrane TNF-alpha mediated NF-kappaB pathway. J. Cell. Mol. Med. *20*, 2318–2327.

Gordon, D.E., Jang, G.M., Bouhaddou, M., Xu, J., Obernier, K., White, K.M., O'Meara, M.J., Rezelj, V.V., Guo, J.Z., Swaney, D.L., et al. (2020). A SARS-CoV-2 protein interaction map reveals targets for drug repurposing. Nature *583*, 459–468.

Hermine, O., Mariette, X., Tharaux, P.L., Resche-Rigon, M., Porcher, R., Ravaud, P., and Group, C.-C. (2021). Effect of tocilizumab vs usual care in adults hospitalized with COVID-19 and moderate or severe pneumonia: a randomized clinical trial. JAMA Intern. Med. *181*, 32–40.

Hoffmann, M., Kleine-Weber, H., Schroeder, S., Kruger, N., Herrler, T., Erichsen, S., Schiergens, T.S., Herrler, G., Wu, N.H., Nitsche, A., et al. (2020). SARS-CoV-2 cell entry depends on ACE2 and TMPRSS2 and is blocked by a clinically proven protease inhibitor. Cell *181*, 271–280.e8.

Kolls, J.K., and Lindén, A. (2004). Interleukin-17 family members and inflammation. Immunity *21*, 467–476.

Kuba, K., Imai, Y., Ohto-Nakanishi, T., and Penninger, J.M. (2010). Trilogy of ACE2: a peptidase in the renin-angiotensin system, a SARS receptor, and a partner for amino acid transporters. Pharmacol. Ther. *128*, 119–128.

Lescure, F.X., Bouadma, L., Nguyen, D., Parisey, M., Wicky, P.H., Behillil, S., Gaymard, A., Bouscambert-Duchamp, M., Donati, F., Le Hingrat, Q., et al. (2020). Clinical and virological data of the first cases of COVID-19 in Europe: a case series. The Lancet. Infect. Dis. *20*, 697–706.

Li, J.Y., Liao, C.H., Wang, Q., Tan, Y.J., Luo, R., Qiu, Y., and Ge, X.Y. (2020). The ORF6, ORF8 and nucleocapsid proteins of SARS-CoV-2 inhibit type I interferon signaling pathway. Virus Res. *286*, 198074.

Li, X., Bechara, R., Zhao, J., McGeachy, M.J., and Gaffen, S.L. (2019). IL-17 receptor-based signaling and implications for disease. Nat. Immunol. *20*, 1594–1602.

Lore, N.I., Bragonzi, A., and Cigana, C. (2016). The IL-17A/IL-17RA axis in pulmonary defence and immunopathology. Cytokine Growth Factor Rev. *30*, 19–27.

Mangalmurti, N., and Hunter, C.A. (2020). Cytokine storms: understanding COVID-19. Immunity *53*, 19–25.

McGeachy, M.J., Cua, D.J., and Gaffen, S.L. (2019). The IL-17 family of cytokines in health and disease. Immunity *50*, 892–906.

McNamara, R.P., Costantini, L.M., Myers, T.A., Schouest, B., Maness, N.J., Griffith, J.D., Damania, B.A., MacLean, A.G., and Dittmer, D.P. (2018). Nef secretion into extracellular vesicles or

exosomes is conserved across human and simian immunodeficiency viruses. mBio *9*, e02344–17.

Mellett, M., Atzei, P., Bergin, R., Horgan, A., Floss, T., Wurst, W., Callanan, J.J., and Moynagh, P.N. (2015). Orphan receptor IL-17RD regulates Toll-like receptor signalling via SEFIR/TIR interactions. Nat. Commun. *6*, 6669.

Mellett, M., Atzei, P., Horgan, A., Hams, E., Floss, T., Wurst, W., Fallon, P.G., and Moynagh, P.N. (2012). Orphan receptor IL-17RD tunes IL-17A signalling and is required for neutrophilia. Nat. Commun. *3*, 1119.

Miorin, L., Kehrer, T., Sanchez-Aparicio, M.T., Zhang, K., Cohen, P., Patel, R.S., Cupic, A., Makio, T., Mei, M., Moreno, E., et al. (2020). SARS-CoV-2 Orf6 hijacks Nup98 to block STAT nuclear import and antagonize interferon signaling. Proc. Natl. Acad. Sci. U S A *117*, 28344–28354.

Mukhamedova, N., Hoang, A., Dragoljevic, D., Dubrovsky, L., Pushkarsky, T., Low, H., Ditiatkovski, M., Fu, Y., Ohkawa, R., Meikle, P.J., et al. (2019). Exosomes containing HIV protein Nef reorganize lipid rafts potentiating inflammatory response in bystander cells. PLoS Pathog. *15*, e1007907.

Nordholm, J., Petitou, J., Ostbye, H., da Silva, D.V., Dou, D., Wang, H., and Daniels, R. (2017). Translational regulation of viral secretory proteins by the 5′ coding regions and a viral RNA-binding protein. J. Cell Biol. *216*, 2283–2293.

Orlov, M., Wander, P.L., Morrell, E.D., Mikacenic, C., and Wurfel, M.M. (2020). A case for targeting Th17 cells and IL-17A in SARS-CoV-2 infections. J. Immunol. https://doi.org/10.4049/jimmunol.2000554.

Pacha, O., Sallman, M.A., and Evans, S.E. (2020). COVID-19: a case for inhibiting IL-17? Nat. Rev. Immunol. *20*, 345–346.

Rao, Y., Wang, T.Y., Qin, C., Espinosa, B., Liu, Q., Ekanayake, A., Zhao, J., Savas, A.C., Zhang, S., Zarinfar, M., et al. (2021). Targeting CTP synthetase 1 to restore interferon induction and impede nucleotide synthesis in SARS-CoV-2 infection. bioRxiv. https://doi.org/10.1101/2021.02.05.429959.

Russell, C.D., Millar, J.E., and Baillie, J.K. (2020). Clinical evidence does not support corticosteroid treatment for 2019-nCoV lung injury. Lancet *395*, 473–475.

Salama, C., Han, J., Yau, L., Reiss, W.G., Kramer, B., Neidhart, J.D., Criner, G.J., Kaplan-Lewis, E., Baden, R., Pandit, L., et al. (2021). Tocilizumab in patients hospitalized with Covid-19 pneumonia. N. Engl. J. Med. *384*, 20–30.

Schwandner, R., Yamaguchi, K., and Cao, Z. (2000). Requirement of tumor necrosis factor receptor-associated factor (TRAF)6 in interleukin 17 signal transduction. J. Exp. Med. *191*, 1233–1240.

Shang, J., Wan, Y., Luo, C., Ye, G., Geng, Q., Auerbach, A., and Li, F. (2020). Cell entry mechanisms of SARS-CoV-2. Proc. Natl. Acad. Sci. U S A *117*, 11727–11734.

Stone, J.H., Frigault, M.J., Serling-Boyd, N.J., Fernandes, A.D., Harvey, L., Foulkes, A.S., Horick, N.K., Healy, B.C., Shah, R., Bensaci, A.M., et al. (2020). Efficacy of tocilizumab in patients hospitalized with Covid-19. N. Engl. J. Med. *383*, 2333–2344.

To, K.K., Tsang, O.T., Leung, W.S., Tam, A.R., Wu, T.C., Lung, D.C., Yip, C.C., Cai, J.P., Chan, J.M., Chik, T.S., et al. (2020). Temporal profiles of viral load in posterior oropharyngeal saliva samples and serum antibody responses during infection by SARS-CoV-2: an observational cohort study. Lancet Infect. Dis. *20*, 565–574.

Vaninov, N. (2020). In the eye of the COVID-19 cytokine storm. Nat. Rev. Immunol. *20*, 277.

Walls, A.C., Park, Y.J., Tortorici, M.A., Wall, A., McGuire, A.T., and Veesler, D. (2020). Structure, function, and antigenicity of the SARS-CoV-2 spike glycoprotein. Cell *181*, 281–292 e286.

Wu, C., Chen, X., Cai, Y., Xia, J., Zhou, X., Xu, S., Huang, H., Zhang, L., Zhou, X., Du, C., et al. (2020). Risk factors associated with acute respiratory distress syndrome and death in patients with coronavirus disease 2019 pneumonia in Wuhan, China. JAMA Intern. Med. https://doi.org/10.1001/jamainternmed.2020.0994.

Yin, Z., Han, Z., Hu, T., Zhang, S., Ge, X., Huang, S., Wang, L., Yu, J., Li, W., Wang, Y., et al. (2020). Neuron-derived exosomes with high miR-21-5p expression promoted polarization of M1 microglia in culture. Brain Behav. Immun. *83*, 270–282.

Young, B.E., Fong, S.W., Chan, Y.H., Mak, T.M., Ang, L.W., Anderson, D.E., Lee, C.Y., Amrun, S.N., Lee, B., Goh, Y.S., et al. (2020). Effects of a major deletion in the SARS-CoV-2 genome on the severity of infection and the inflammatory response: an observational cohort study. Lancet *396*, 603–611.

Zhang, C., Shi, L., and Wang, F.S. (2020a). Liver injury in COVID-19: management and challenges. The lancet. Gastroenterol. Hepatol. *5*, 428–430.

Zhang, Y., Zhang, J., Chen, Y., Luo, B., Yuan, Y., Huang, F., Yang, T., Yu, F., Liu, J., Liu, B., et al. (2020b). The ORF8 protein of SARS-CoV-2 mediates immune evasion through potently downregulating MHC-I. bioRxiv. https://doi.org/10.1101/2020.05.24.111823.

iScience, Volume *24*

Supplemental information

ORF8 contributes to cytokine storm during SARS-CoV-2 infection by activating IL-17 pathway

Xiaoyuan Lin, Beibei Fu, Songna Yin, Zhifeng Li, Huawen Liu, Haiwei Zhang, Na Xing, Yu Wang, Weiwei Xue, Yan Xiong, Shanfu Zhang, Qingting Zhao, Shiyao Xu, Jing Zhang, Peihui Wang, Weiqi Nian, Xingsheng Wang, and Haibo Wu

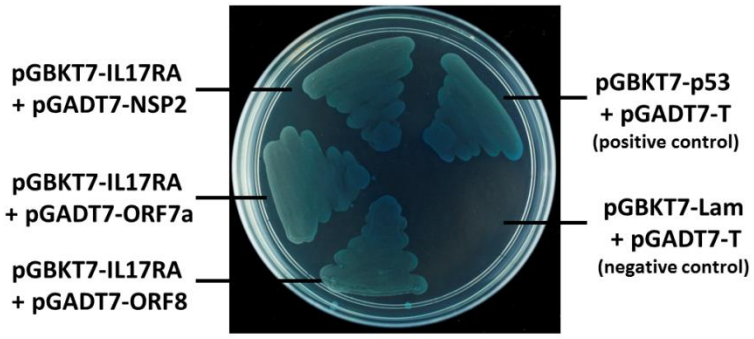

Figure S1 **NSP2, ORF7a and ORF8 are the potential candidates that interacts with IL17RA. Related to Figure 1.**

Positive clones obtained by yeast two-hybrid screening. pGBKT7-p53+pGADT7-T: positive control; pGBKT7-Lam+pGADT7-T: negative control.

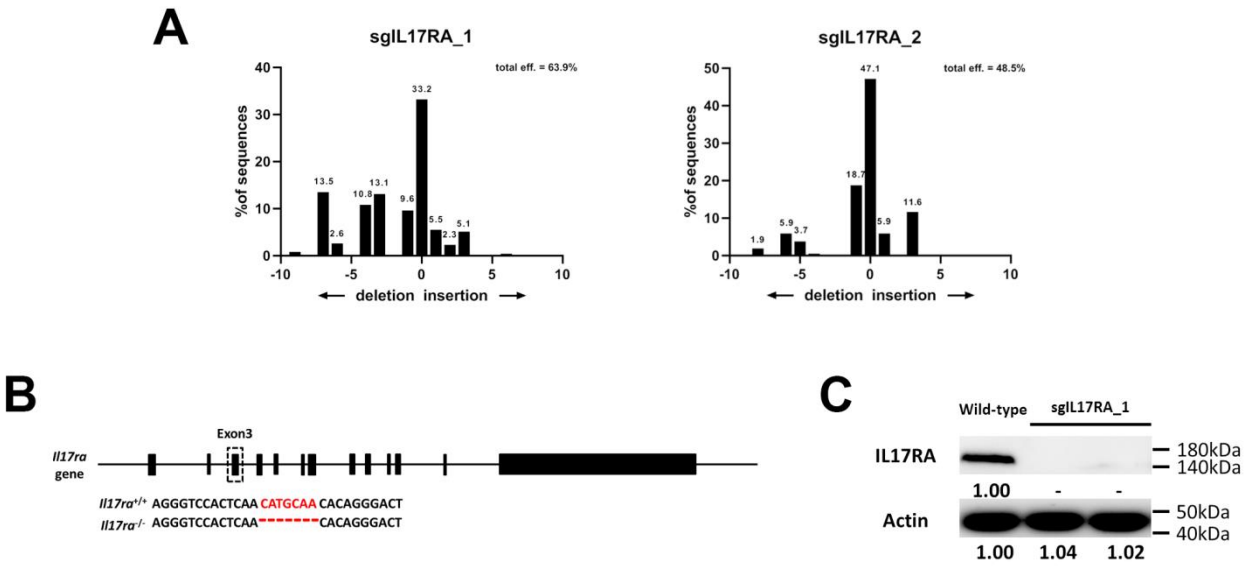

Figure S2 **Validation of *Il17ra*-deficient RAW264.7 cells. Related to Figure 1.**

(A) TIDE analysis of *Il17ra*$^{-/-}$ RAW264.7 cell pools produced by sgRNA1 and sgRNA2. (B) Schematic illustration of the target region of *Il17ra*$^{-/-}$ RAW264.7 cell clone. (C) IL17RA expression in *Il17ra*$^{-/-}$ RAW264.7 cell clone was analyzed by Western Blotting. The clone was derived from the cell pool produced by sgRNA1. Data are representative of three independent experiments (C).

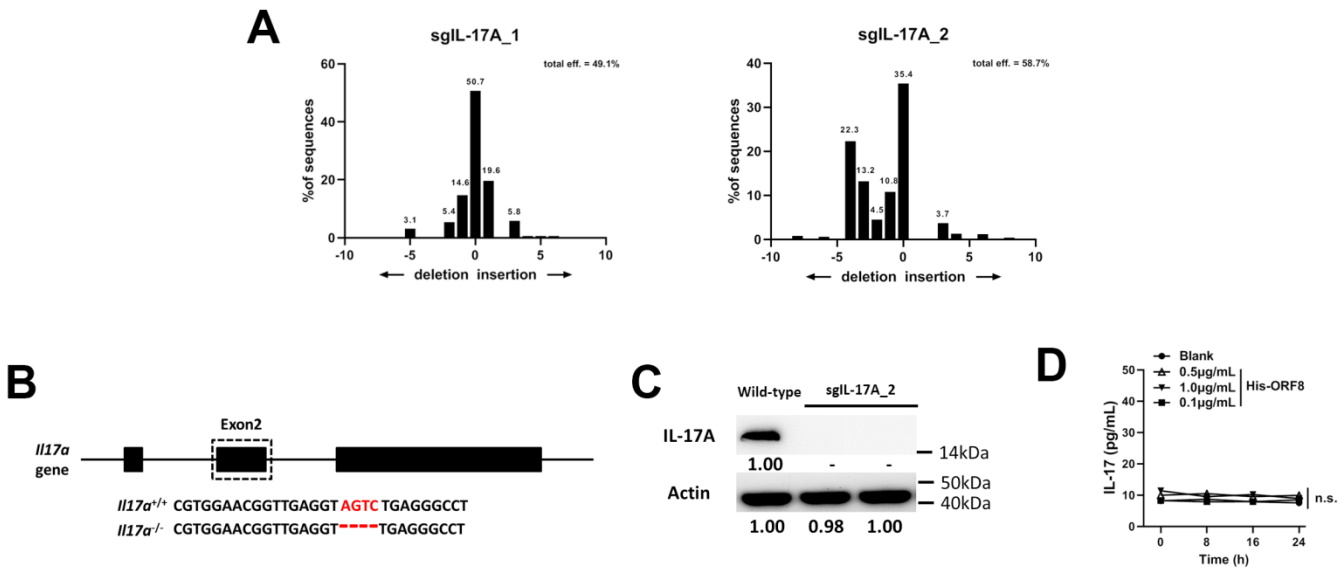

Figure S3 **Validation of *Il17a*-deficient RAW264.7 cells. Related to Figure 1.**

(A) TIDE analysis of *Il17a*$^{-/-}$ RAW264.7 cell pools produced by sgRNA1 and sgRNA2. (B) Schematic illustration of the target region of *Il17a*$^{-/-}$ RAW264.7 cell clone. (C) IL-17A expression in *Il17a*$^{-/-}$ RAW264.7 cell clone was analyzed by Western Blotting. The clone was derived from the cell pool produced by sgRNA2. (D) His-ORF8 was added to culture media of *Il17a*$^{-/-}$ RAW264.7 cells, and IL-17 expression was analyzed by ELISA. Data are representative of three independent experiments (C) or three independent experiments with n = 3 technical replicates (D) (shown as mean ± s.e.m. in D). Data are analyzed by two-tailed Student *t* test (D). Abbreviations: n.s., not significant.

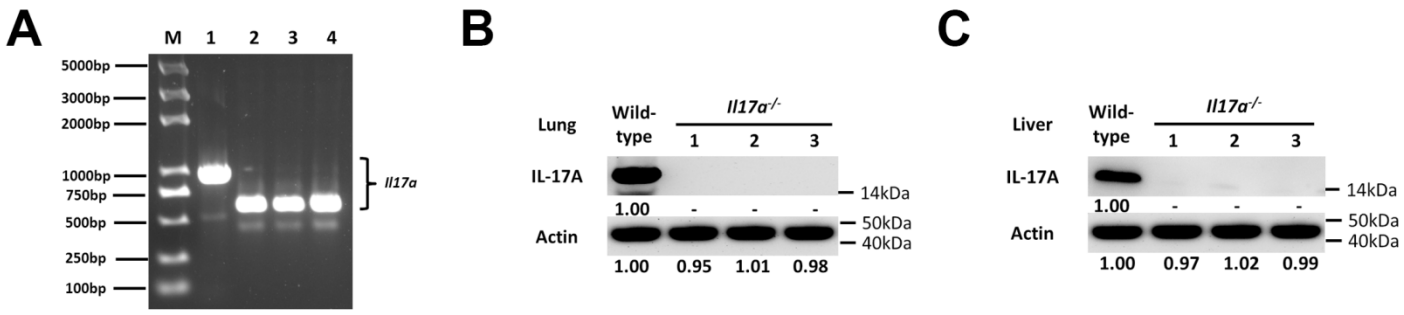

Figure S4 **Validation of *Il17a*-deficient mice. Related to Figure 2.**

(A) IL-17A expression in *Il17a*-deficient mice was analyzed by gel electrophoresis. M: marker; 1: wild-type mice; 2-4: *Il17a*-deficient mice. (B-C) IL-17A expression in lungs (B) and livers (C) of *Il17a*-deficient mice. Data are representative of three independent experiments.

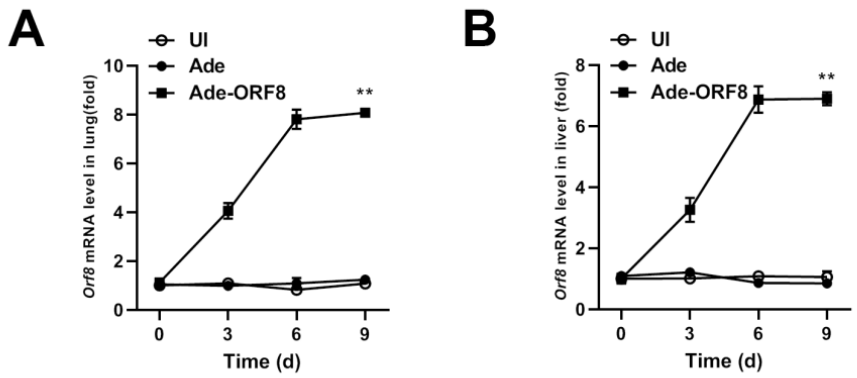

Figure S5 **Adenovirus-mediated ORF8 expression in mice. Related to Figure 2.**

(A-B) ORF8 expression in lungs (A) and livers (B) of *Il17a*-deficient mice after injection of Ade-ORF8. UI: uninfection. Data are representative of three independent experiments with n = 3 technical replicates (shown as mean ± s.e.m.). Data are analyzed by two-tailed Student *t* test. **, $p < 0.01$.

Transparent Methods

Ethic statement

This study was carried out in accordance with the Guidelines for the Care and Use of Animals of Chongqing University. All animal experimental procedures were approved by the Animal Ethics Committees of the School of Life Sciences, Chongqing University.

Mice

Six- to eight-week-old wild-type C57BL/6 mice and *Il17a*-deficient mice (C57BL/6N-Il17a^{em1cyagen}) were purchased from Cyagen Biosciences (Guangzhou, China). Mice used in each experiment were half male and half female, and age- and sex- matched in experimental group and control group. All animal study protocols were reviewed and approved by Chongqing University School of Life Sciences review boards for animal studies. The upstream and downstream primers were designed on exon 1 and exon 3 of mouse *Il17a* (NM_010552) (F-GCAAACATGAGTCCAGG, R-TGGTTTTCACCCCATTC). Three knockout mice were randomly selected to extract genomic DNA, and PCR was used to detect the length of the knockout fragment (~212bp). Meanwhile, lung and liver were taken to detect IL17RA expression by Western Blotting.

Plasmids construction

Full-length coding sequence (CDS) of SARS-CoV-2 NSP2, ORF7a and ORF8 (NCBI

Accession number: NC_045512.2) were synthesized by Beijing Genomics Institute (BGI, Beijing, China). NSP2, ORF7a, or ORF8 CDS was inserted into pCMV-HA (for eukaryotic expression) or pET-28a (+) (for protein production and purification), respectively. For GST pulldown assay, ORF8 CDS was inserted into pGEX-4T-1. Full-length CDS of IL17RA (NCBI Accession number: NM_008359.2) was inserted into pCMV-Myc. Primers are as follows: F-AATTGTCGACTATGGCGATTCGG, R-ATAAGCGGCCGCCCAAATGTCTGAT. The pNL3.2.NF-κB-RE plasmid used in the measurement of NF-κB activity was purchased from Promega (Madison, WI, USA).

Yeast two-hybrid screening

Yeast two-hybrid screening was performed using the Matchmaker Gold Yeast Two-Hybrid System (Takara, Dalian, China). Briefly, a SARS-CoV-2 protein expressing library was constructed by using the Make Your Own "Mate & Plate" Library System (Takara) strictly according to the manufacturer's instructions. Then the library was cloned to a yeast Gal4 activation domain (AD) vector pGADT7, and transformed into yeast strain Y187 to serve as "prey"; IL17RA cDNA was cloned to a Gal4 binding domain (BD) vector pGBKT7, and transformed into yeast strain Y2HGold to serve as "bait". Prey and bait were combined together to screen for positive interactions. Colonies grown on the synthetic defined (SD) plate lacking adenine, histidine, leucine, and tryptophan (SD/-Ade-His-Leu-Trp) were picked for Sanger sequencing (Supplemental File Sets).

Protein production and purification

Production and purification of ORF8, NSP2, or ORF7a protein were performed as follows(Walls et al., 2020): pET-28a(+)-ORF8, pET-28a(+)-NSP2, or pET-28a(+)-ORF7a construct was transformed into *E. coli* BL21 (DE3) and cultured in LB media at 37 °C until OD600 reached 0.6. The recombinant expression of His-tagged protein was induced by adding isopropyl β-D-thiogalactoside (IPTG) with a final concentration of 125 μM and stimulating for 16 h at 12 °C. Cells were harvested by centrifugation at 4 °C, and lysed by freezing/thawing method. Purification of the supernatants containing His-tagged protein was performed by Ni-affinity chromatography in an ÄKTA Primer FPLC system (GE Healthcare Life Sciences, Chicago, IL, USA) using the HisTrap FF columns (GE Healthcare Life Sciences) according to the manufacturer's instructions.

Cell culture and treatment

HEK293T cells were purchased from American Type Culture Collection (ATCC, Manassas, VA, USA). The culture medium was composed of Dulbecco's Modified Eagle's Medium (DMEM, Gibco, San Jose, CA, USA) and 10% fetal bovine serum (Gibco). Plasmid DNA was transfected into indicated cells using Lipofectamine 3000 Transfection Reagent (Invitrogen, Life Technologies, CA, USA) according to the manufacturer's instructions. *Il17ra*$^{-/-}$ and *Il17a*$^{-/-}$ RAW264.7 were generated using CRISPR-Cas9. To be detailed, two sgRNAs were designed for each gene

(*Il17ra*-sgRNA1: TCCACTCAACATGCAACACA; *Il17ra*-sgRNA2: GGGGGTGGATTCATTCCACA; *Il17a*-sgRNA1: CTCAGCGTGTCCAAACACTG; *Il17a*-sgRNA2: GAACGGTTGAGGTAGTCTGA), and ligated into pSpCas9(BB)-2A-Puro (PX459) after being digested by Bbs I. The recombinant was then transfected into RAW264.7 (ATCC) using Lipo 3000 Transfection Reagent (Invitrogen). After 48 h, DMEM containing 3 μg/mL puromycin was used for screening for 7 days to obtain the cell pool. Half of the cells were taken for TIDE analysis (http://shinyapps.datacurators.nl/tide/), and the remaining cells were used for limiting dilution to obtain the cell clone. Genomic DNA was extracted and sequenced, and the indels were analyzed. For the obtained homozygous knockout monoclone, total cell protein was extracted and Western Blotting was used to detect expressions of IL17RA and IL-17A. *Il17ra*$^{+/+}$ PMs were isolated as follows(Kim et al., 2016) : mice were intraperitoneally injected with HBSS containing 2 mM EDTA and 2% FBS. After flushing the abdominal cavity, 5 ml of flushing solution was collected and centrifuged 10 min at 400×g, 4°C. Supernatant was discarded and cell pellet was resuspended in cold DMEM/F12. The cells were cultured at 37°C for 2 h and attached to the substrate. The nonadherent cells were removed by gently washing with warm PBS three times. The purified PMs were plated at a density of 1×10^6 cells/60 mm plastic dish. Afterwards, purified NSP2, ORF7a, or ORF8 was added to culture media of *Il17ra*$^{+/+}$ PMs for treatment. After 24 h, cells were harvested for immunoprecipitation. In addition, purified ORF8 was added to culture media of *Il17ra*$^{-/-}$ RAW264.7 or *Il17a*$^{-/-}$ RAW264.7 for treatment. After 24 h, cells were

harvested for immunoprecipitation.

GST pulldown assay

GST pulldown assay was performed using the GST Protein Interaction Pull-Down Kit (Thermo Fisher Scientific, San Jose, CA, USA) following the manufacturer's instructions. Briefly, the glutathione-S-transferase (GST)-tagged SARS-CoV-2 ORF8 fusion proteins were expressed in *Escherichia coli* (*E. coli*) and immobilized on the glutathione agarose resin, and then incubated with HEK293T cell lysates transfected with pCMV-Myc-IL17RA. After incubation at 4°C for at least 4 h (overnight if possible) with gentle rocking motion on a rotating platform, elution was collected for detection of protein interaction by Western Blotting.

Immunoblot and Immunoprecipitation

Immunoblot analysis was performed as follows(Fu et al., 2020) : total proteins were collected and separated by SDS-PAGE, and transferred to PVDF membrane. Blots were probed with 1/1000 anti-Actin (AF5001), 1/1000 anti-GST (AF2299) (Beyotime, Shanghai, China), 1/1000 anti-HA (SAB2702196), 1/1000 anti-Myc (SAB2702192) (Sigma-Aldrich, St. Louis, MO, USA), 1/200 anti-IL-17 (sc-374218) (Santa Cruz Biotechnology, Santa Cruz, CA, USA), 1/200 anti-IL17RA (PA5-47199), 1/200 anti-ACT1 (14-4040-82) (Invitrogen), 1/200 anti-phospho-IκBα (Ser32/36) (9246), 1/500 anti-IκBα (9242) (Cell Signaling Technology, Inc., Danvers, MA, USA) antibodies. Co-immunoprecipitation was performed according to previous studies

(Lafont et al., 2018; Su et al., 2019). Briefly, cells were harvested and lysed with RIPA Lysis Buffer (50 mM Tris (pH 7.4), 150 mM NaCl, 1% Triton X-100, 1% sodium deoxycholate, 0.1% SDS) (P0013B, Beyotime) containing protease inhibitor cocktail. Cell lysate was centrifuged at 12, 000×g for 10 min. Part of the supernatant was taken to determine the total protein concentration and used as the input for immunoblotting, and the remaining supernatant was incubated with appropriate antibodies and Protein A/G beads (Thermo Fisher Scientific) overnight at 4°C. Precipitated protein complex was mixed with 5× SDS Loading Buffer and boiled at 98°C for 8 min, followed by immunoblotting with indicated antibodies.

NF-κB activity assay

Dual Luciferase Reporter (DLR) Assay System (Promega) was used to perform NF-κB activity assays as follows(Fu et al., 2020) : firefly luciferase plasmid pNL3.2.NF-κB-RE and Renilla luciferase plasmid pRL-SV40 (internal control) were co-transfected to cells. Twenty-four h after treatment or stimulation, cell lysates were harvested for DLR assays. Data were collected with a VICTOR X5 Multilabel Plate Reader (PerkinElmer, Waltham, MA, USA). The relative NF-κB activity was measured by Firefly luciferase luminescence divided by Renilla luciferase luminescence.

Exposure of mice to adenoviral vectors

The construction and characterization of recombinant adenovirus vector encoding

SARS-CoV-2 ORF8 (Ade-ORF8) were referred as follows(Huang et al., 2019): the CDS of ORF8 was cloned into pENTR™/D-TOPO vector (Thermo Fisher Scientific) followed by recombination into the pAd/CMV/V5-DEST (Thermo Fisher Scientific). The replication-deficient recombinant Ade-ORF8 adenovirus was produced in HEK293A cells. Mice were anesthetized, and then intratracheally instilled with Ade-ORF8 at 10^8 PFU/mouse diluted in 50 μL PBS.

IL17RA blocking

Anti-mouse IL17RA antibody (MAB4481) and mouse IgG1 isotype control (MAB002) were purchased from R&D Systems. For injections, antibody stocks were diluted in sterile PBS and each mouse received 200 μg per injection.

H&E staining

On the 9^{th} day after infection, the lung and liver of mice were fixed with 10% buffered formaldehyde for more than 24 h, embedded in paraffin, sectioned, and stained with H&E according to the standard procedure. Photographs were obtained by microscope (Carl Zeiss, Jena, Germany). A scoring system was set as follows (Kleiner et al., 2005; Matute-Bello et al., 2011) : five fields at 200× magnification were randomly selected for each slice. The lung scoring criteria are as follows: 0, pulmonary lobes lacked lesions; 1, multifocal lesions with mild lymphocyte and macrophage infiltration; 2, mild infiltration of peri-bronchial, peri-vascular and alveolar; 3, small range of blocked terminal bronchioles, fibroplasia or organization; 4, wide range of alveolar

necrosis and hyaline thrombus. The liver scoring criteria are as follows: 0, hepatic lobules lacked lesions; 1, scattered inflammation with ≤3 lesions in hepatic lobules; 2, 3-7 lesions in hepatic lobules, accounting for＜1/3 of the hepatic lobule; 3, scattered inflammation with＞7 lesions, accounting for 1/3-2/3 of the hepatic lobule; 4, inflammatory lesions spread throughout hepatic lobules, with large areas of hepatocyte necrosis.

Enzyme-linked immunosorbent assay (ELISA)

Mouse TNF-α, IL-1β, IL-6, IL-12 ELISA kits were purchased from BD Biosciences (Franklin Lakes, NJ, USA). Cell culture supernatants were assayed according to the manufacturer's protocols. Mice were sacrificed and lungs/livers were quickly excised, rinsed of blood, and homogenized by adding 1 mL homogenization buffer (PBS containing 0.05% sodium azide, 0.5% Triton X-100, and a protease inhibitor cocktail, pH 7.2, 4˚C), and then sonicated for 10 minutes. Homogenates were centrifuged at 12,000×g for 10 minutes, and the supernatant was taken to determine the total protein concentration, followed by ELISA analysis. The concentration of each cytokine was calculated against a standard curve.

Statistical analysis

Two-tailed Student's *t* test was used to compare the means between two groups. A value of $P < 0.05$ was considered significant.

Supplemental References

Fu, B., Yin, S., Lin, X., Shi, L., Wang, Y., Zhang, S., Zhao, Q., Li, Z., Yang, Y., and Wu, H. (2020). PTPN14 aggravates inflammation through promoting proteasomal degradation of SOCS7 in acute liver failure. Cell death & disease *11*, 803.

Huang, J., Snook, A.E., Uitto, J., and Li, Q. (2019). Adenovirus-Mediated ABCC6 Gene Therapy for Heritable Ectopic Mineralization Disorders. The Journal of investigative dermatology *139*, 1254-1263.

Kim, K.W., Williams, J.W., Wang, Y.T., Ivanov, S., Gilfillan, S., Colonna, M., Virgin, H.W., Gautier, E.L., and Randolph, G.J. (2016). MHC II+ resident peritoneal and pleural macrophages rely on IRF4 for development from circulating monocytes. The Journal of experimental medicine *213*, 1951-1959.

Kleiner, D.E., Brunt, E.M., Van Natta, M., Behling, C., Contos, M.J., Cummings, O.W., Ferrell, L.D., Liu, Y.C., Torbenson, M.S., Unalp-Arida, A., et al. (2005). Design and validation of a histological scoring system for nonalcoholic fatty liver disease. Hepatology *41*, 1313-1321.

Lafont, E., Draber, P., Rieser, E., Reichert, M., Kupka, S., de Miguel, D., Draberova, H., von Massenhausen, A., Bhamra, A., Henderson, S., et al. (2018). TBK1 and IKKepsilon prevent TNF-induced cell death by RIPK1 phosphorylation. Nature cell biology *20*, 1389-1399.

Matute-Bello, G., Downey, G., Moore, B.B., Groshong, S.D., Matthay, M.A., Slutsky, A.S., Kuebler, W.M., and Acute Lung Injury in Animals Study, G. (2011). An official American Thoracic Society workshop report: features and measurements of experimental acute lung injury in animals. American journal of respiratory cell and molecular biology *44*, 725-738.

Su, Y., Huang, J., Zhao, X., Lu, H., Wang, W., Yang, X.O., Shi, Y., Wang, X., Lai, Y., and Dong, C. (2019). Interleukin-17 receptor D constitutes an alternative receptor for interleukin-17A important in psoriasis-like skin inflammation. Science immunology *4*.

Walls, A.C., Park, Y.J., Tortorici, M.A., Wall, A., McGuire, A.T., and Veesler, D. (2020). Structure, Function, and Antigenicity of the SARS-CoV-2 Spike Glycoprotein. Cell *181*, 281-292 e286.